1996

Critical properties of the one-dimensional spin- ½ antiferromagnetic Heisenberg model in the presence of a uniform field

A. Fledderjohann

C. Gerhardt

K. H. Mütter

A. Schmitt

M. Karbach
University of Rhode Island

Citation/Publisher Attribution

Fledderjohann, A., Gerhardt, C., Mütter, K. H., Schmitt, A., & Karbach, M. (1996). Critical properties of the one-dimensional spin- ½ antiferromagnetic Heisenberg model in the presence of a uniform field. *Phys. Rev. B., 54*, 7168-7176. doi: 10.1103/PhysRevB.54.7168
Available at: https://doi.org/10.1103/PhysRevB.54.7168

Critical properties of the one-dimensional spin-$\frac{1}{2}$ antiferromagnetic Heisenberg model in the presence of a uniform field

A. Fledderjohann, C. Gerhardt, K. H. Mütter,* and A. Schmitt
Department of Physics, University of Wuppertal, D-42097 Wuppertal, Germany

M. Karbach
Department of Physics, The University of Rhode Island, Kingston, Rhode Island 02881

(Received 12 April 1996)

In the presence of a uniform field the one-dimensional spin-$\frac{1}{2}$ antiferromagnetic Heisenberg model develops zero frequency excitations at field-dependent ''soft-mode'' momenta. We determine three types of critical quantities, which we extract from the finite-size dependence of the lowest excitation energies, the singularities in the static structure factors and the infrared singularities in the dynamical structure factors at the soft mode momenta. We also compare our results with the predictions of conformal field theory. [S0163-1829(96)08734-6]

I. INTRODUCTION

In this paper we are going to study the zero-temperature dynamics of the one-dimensional spin-$\frac{1}{2}$ antiferromagnetic Heisenberg model

$$H \equiv 2\sum_{x=1}^{N} \vec{S}(x)\vec{S}(x+1) - 2B\sum_{x=1}^{N} S_3(x) \tag{1.1}$$

in the presence of a uniform external field B. The quantities of interest are the dynamical structure factors at fixed magnetization $M \equiv S/N$:

$$S_a(\omega,p,M,N) = \sum_n \delta[\omega-(E_n-E_s)]|\langle n|S_a(p)|s\rangle|^2,$$

$$a=3,+,-. \tag{1.2}$$

They are defined by the transition probabilities $|\langle n|S_a(p)|s\rangle|^2$ from the ground states $|s\rangle \equiv |S,S_3=S\rangle$ in subspaces with total spin S and energy E_s to the excited states $|n\rangle$ with energy E_n. The transition operators we are concerned with are the Fourier transforms of the single-site spin operators $S_a(x)$,

$$S_a(p) \equiv \frac{1}{\sqrt{N}}\sum_{x=1}^{N} e^{ipx} S_a(x), \quad a=3,+,-. \tag{1.3}$$

The structure factors (1.2) have been investigated previously by Müller *et al.*[1] They performed a complete diagonalization of the Hamiltonian (1.1) on small systems ($N \leqslant 10$), and analyzed the spin-wave continua by approximately solving the Bethe ansatz equations for the low-lying excitations. In particular, they found a lower bound

$$\omega \geqslant |\omega_3(p,M)|, \tag{1.4}$$

$$\omega_3(p,M) = 2D\sin\frac{p}{2}\sin\frac{p-p_3(M)}{2} \tag{1.5}$$

for the excitations contributing to the longitudinal structure factor $S_3(\omega,p,M)$. The constant D on the right-hand side of (1.5) is fixed by the magnetization curve[2]

$$B(M) = 2D\sin\pi M. \tag{1.6}$$

The lower bound vanishes at $p=0$ and at the field-dependent momentum

$$p_3(M) = \pi(1-2M), \tag{1.7}$$

signaling the emergence of zero-frequency modes (soft modes) in the spectrum of excitation energies. The analysis of the spin-wave continua relevant for the transverse structure factors $S_\pm(\omega,p,M)$ leads to the approximate lower bounds

$$\omega \geqslant \omega_\pm(p,M), \tag{1.8}$$

for the excitations produced by the raising and lowering operators $S_+(p), S_-(p)$, respectively:

$$\omega_+(p,M) = 2D\left[\sin\frac{p}{2}\cos\left(\frac{p}{2}-\pi M\right) - \sin\pi M\right]$$

for

$$p_1(M) \leqslant p \leqslant \pi \tag{1.9}$$

and

$$\omega_-(p,M) = |\omega_3(\pi-p,M)| \quad \text{for } 0 \leqslant p \leqslant \pi. \tag{1.10}$$

Both bounds vanish at $p=\pi$ and at $p=p_1(M)=2\pi M$. The soft modes at the field-dependent momenta $p_j(M)$, $j=1$ and 3, produce characteristic structures in the momentum dependence of the corresponding static structure factors.[3,4] It is the purpose of this paper to analyze singularities in the static structure factors, and infrared singularities in the dynamical structure factors (1.2) at the soft-mode momenta. In Sec. II we review our method to compute the excitation energies and transition probabilities for finite rings ($N \leqslant 36$). The finite-size dependence of the lowest excitation energy at the soft mode momenta is analyzed by solving the Bethe ansatz

TABLE I. Energies and transition probabilities for the lowest excitations in the transverse structure factor $S_-(\omega,p,M,N)$ for $M=\frac{1}{4}$, and $N=16$, $p=\pi$ (left-hand part); and $p_-=\pi/2-2\pi/16$ (right-hand part). The upper and lower parts in the table contain the results of an exact diagonalization and the recursion method, respectively.

$S_-(\tau=0,p=\pi)=2.523\,604\,278\,922\,20$		$S_-(\tau=0,p=p_-)=5.013\,848\,769\,698\,94\times10^{-1}$		
$\omega_n(\pi)$	$w_n(\pi)$	$\omega_n(p_-)$	$w_n(p_-)$	
0.244 903 181 204 07	$7.695\,433\,363\,399\,13\times10^{-1}$	0.876 103 276 253 77	$1.954\,987\,610\,124\,65\times10^{-1}$	*
2.000 624 236 617 84	$9.814\,682\,018\,286\,58\times10^{-2}$	2.509 396 243 236 48	$5.594\,000\,643\,834\,86\times10^{-2}$	
3.162 714 788 205 13	$2.645\,725\,074\,408\,14\times10^{-4}$	3.473 984 785 232 09	$6.945\,758\,289\,762\,92\times10^{-3}$	
3.578 650 171 744 11	$6.853\,045\,073\,523\,09\times10^{-3}$	3.603 249 228 192 52	$9.821\,628\,583\,478\,71\times10^{-4}$	
3.980 619 720 787 59	$4.713\,901\,191\,664\,36\times10^{-2}$	3.713 270 710 282 90	$8.014\,159\,463\,064\,66\times10^{-2}$	
4.352 696 524 991 91	$9.627\,111\,596\,805\,98\times10^{-5}$	4.214 054 148 294 30	$2.865\,647\,260\,321\,45\times10^{-4}$	
4.729 943 842 646 68	$8.688\,809\,239\,198\,77\times10^{-4}$	4.170 339 854 626 45	$7.714\,555\,418\,915\,09\times10^{-2}$	
5.112 245 989 300 47	$4.946\,920\,330\,047\,24\times10^{-4}$	4.306 160 243 214 60	$2.501\,483\,219\,298\,65\times10^{-2}$	
5.259 958 354 631 19	$3.778\,430\,154\,397\,37\times10^{-5}$	4.399 600 774 592 70	$1.180\,633\,402\,366\,13\times10^{-3}$	
5.453 186 955 024 60	$7.320\,760\,782\,290\,36\times10^{-3}$	4.779 417 562 570 73	$7.947\,471\,971\,000\,13\times10^{-3}$	
5.742 238 217 304 04	$3.486\,978\,636\,107\,70\times10^{-2}$	4.991 533 660 936 31	$5.419\,697\,079\,217\,73\times10^{-6}$	
6.142 234 177 714 73	$2.739\,406\,641\,977\,73\times10^{-6}$	5.100 457 413 216 37	$5.507\,304\,902\,798\,44\times10^{-2}$	
6.203 717 051 547 30	$2.049\,482\,726\,629\,71\times10^{-4}$	5.250 087 787 897 24	$6.305\,399\,859\,183\,68\times10^{-2}$	
6.287 195 281 196 78	$7.304\,078\,086\,745\,98\times10^{-4}$	5.376 160 003 775 36	$7.355\,758\,177\,222\,71\times10^{-4}$	
6.383 874 044 845 64	$1.682\,084\,007\,360\,76\times10^{-5}$	5.469 637 280 712 08	$1.833\,312\,377\,348\,51\times10^{-1}$	*
6.564 066 124 982 08	$1.690\,231\,998\,059\,61\times10^{-2}$	5.487 680 193 617 61	$1.770\,040\,855\,588\,57\times10^{-6}$	
6.769 643 306 484 90	$1.810\,726\,846\,334\,99\times10^{-7}$	5.703 409 466 350 26	$3.361\,983\,377\,347\,69\times10^{-6}$	
6.794 958 978 768 59	$8.477\,376\,822\,003\,00\times10^{-3}$	5.711 491 865 604 78	$3.444\,856\,331\,653\,34\times10^{-2}$	
6.815 339 154 894 40	$3.058\,251\,618\,980\,85\times10^{-5}$	5.780 887 269 704 25	$1.070\,710\,792\,672\,98\times10^{-4}$	
6.830 026 863 400 33	$9.957\,905\,849\,211\,62\times10^{-4}$	5.895 735 704 493 84	$1.380\,330\,537\,225\,50\times10^{-1}$	*
$S_-(\tau=0,p=\pi)=2.523\,604\,278\,923\,49$		$S_-(\tau=0,p=p_-)=5.013\,848\,769\,705\,01\times10^{-1}$		
$\omega_n(\pi)$	$w_n(\pi)$	$\omega_n(p_-)$	$w_n(p_-)$	
0.244 903 181 204 08	$7.695\,433\,363\,395\,20\times10^{-1}$	0.876 103 276 253 76	$1.954\,987\,610\,122\,22\times10^{-1}$	*
2.000 624 236 617 91	$9.814\,682\,018\,281\,77\times10^{-2}$	2.509 396 243 236 56	$5.594\,000\,643\,828\,91\times10^{-2}$	
3.162 714 788 204 83	$2.645\,725\,075\,263\,20\times10^{-4}$	3.473 985 466 693 44	$6.945\,942\,947\,964\,92\times10^{-3}$	
3.578 650 171 737 75	$6.853\,045\,072\,385\,61\times10^{-3}$	3.603 434 615 393 55	$9.858\,170\,673\,307\,08\times10^{-4}$	
3.980 619 720 664 78	$4.713\,901\,185\,295\,35\times10^{-2}$	3.713 275 740 769 44	$8.013\,879\,790\,435\,92\times10^{-2}$	
4.352 694 258 890 94	$9.626\,931\,152\,412\,92\times10^{-5}$	4.170 721 017 669 60	$7.789\,640\,971\,330\,79\times10^{-2}$	
4.729 942 332 777 89	$8.688\,919\,125\,175\,11\times10^{-4}$	4.311 234 173 060 11	$2.563\,192\,362\,225\,87\times10^{-2}$	
5.113 525 671 195 04	$5.062\,605\,748\,090\,40\times10^{-4}$	4.777 307 133 519 60	$8.296\,132\,141\,156\,95\times10^{-3}$	
5.451 596 877 607 25	$7.285\,531\,240\,031\,79\times10^{-3}$	5.129 265 354 985 99	$8.404\,108\,705\,622\,40\times10^{-2}$	
5.741 618 702 167 59	$3.486\,620\,204\,790\,76\times10^{-2}$	5.418 372 489 214 89	$1.834\,871\,713\,305\,98\times10^{-1}$	*
6.105 752 469 338 84	$3.840\,802\,147\,539\,84\times10^{-4}$	5.668 799 489 069 28	$8.773\,679\,984\,736\,76\times10^{-2}$	
6.511 959 824 206 24	$1.067\,767\,162\,920\,14\times10^{-2}$	5.944 244 724 155 45	$1.419\,057\,704\,675\,91\times10^{-1}$	*

equations on large systems ($N\leqslant 2048$). The critical behavior of the static structure factors at the soft-mode momenta $p=p_a(M)$, $a=1$ and 3 and fixed magnetization $M=\frac{1}{4}$ is investigated in Sec. III based on a numerical computation of the ground state on rings with $N=12,16,\ldots,32,36$ sites. In Sec. IV, we demonstrate how infrared singularities emerge in a finite-size scaling analysis of the dynamical structure factors in the Euclidean time representation. Finally, in Sec. V we compare our numerical results with the predictions of conformal field theory.

II. SOFT MODES IN THE EXCITATION SPECTRUM

An approximate scheme to determine low-lying excitation energies and transition probabilities has been proposed in Ref. 5. It starts from the recursion algorithm,[6] which generates a tridiagonal matrix. Eigenvalues and eigenvectors of this matrix yield the exact excitation energies and transition probabilities. There are, however, two sources of numerical errors in this scheme. The orthogonality of the states produced by the recursion algorithm is lost more and more with an increasing number of steps, due to rounding errors. Moreover, the iteration has to be truncated before the Hilbert space is exhausted.

Nevertheless the method yields good results for the lowest 10 excitations—provided that these contain the dominant part of the spectral distribution. This condition is satisfied for the excitations in $S_a(\omega,p,M,N)$, $a=3,+$. For $S_-(\omega,p,M,N)$ near the soft-mode momentum $p_1(M)$, however, this is not the case. In Table I we compare the low-lying excitations for $S_-(\omega,p,M,N)$, $M=\frac{1}{4}$, $p=\pi$, and $p=\pi/2-2\pi/16$ on a ring with $N=16$ sites, as they follow

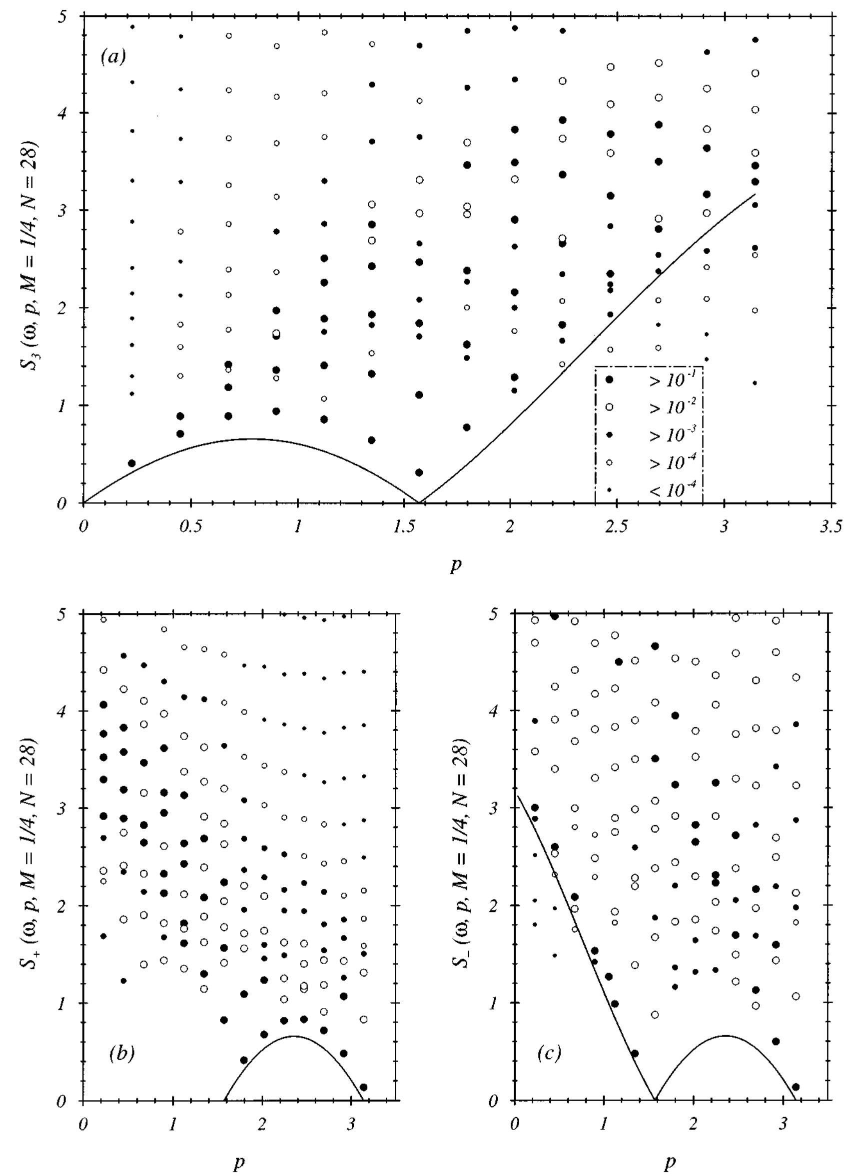

FIG. 1. Momentum dependence of the excitation energies in the dynamical structure factors at $M=\frac{1}{4}$: (a) $S_3(\omega,p,M=\frac{1}{4},\ N=28)$, and (b) $S_+(\omega,p,M=\frac{1}{4},\ N=28)$, and (c) $S_-(\omega,p,M=\frac{1}{4},\ N=28)$. The relative spectral weight is characterized by the different symbols.

from an exact diagonalization (upper part of Table I) and the recursion algorithm (lower part of Table I), respectively.

At $p=\pi$, 76.95% of the spectral weight is found in the first excitation. The energy and relative spectral weight of the first excitation are reproduced within 13 digits. The following seven excitations can be identified term by term with decreasing accuracy for the energies and the relative spectral weights.

The situation is different for $p_-=\pi/2-2\pi/16$, which can be seen in the right hand part of Table I. The exact result yields large spectral weights—marked by an asterisk—for the first (19.55%), the fifteenth (18.33%), and the twentieth (13.80%) excitations. The recursion method reproduces the energy and spectral weight of the first excitation within 13 digits. The two other excitations with large spectral weight—marked by an asterisk—are only in rough agreement with the exact result. We found, however, that this inaccuracy has no effect on the dynamical structure factors in the Euclidean time representation (4.1). The latter will be investigated in Sec. IV. In Figs. 1(a), 1(b), and 1(c), we present the momentum dependence of the excitation energies in the dynamical structure factors $S_a(\omega,p,M=1/4,\ N=28)$ as they follow from the recursion method. The size of the symbols measures the relative spectral weight $w_n\equiv|\langle n|S_a(p)|s\rangle|^2/S_a(p,M,N)$. The normalization is given by the static structure factors

$$S_a(p,M,N)=\int_{\omega_a(p,M,N)}^{\infty} d\omega S_a(\omega,p,M,N), \quad a=3,+,-. \tag{2.1}$$

There is a strict relation between the static transverse structure factors,

$$S_-(p,M,N)=S_+(p,M,N)+2M. \tag{2.2}$$

It should be noted that $S_+(p,M,N)\approx 0$ for $p<p_1(M)$ [cf. Fig. 3(b)], which implies that the absolute spectral weight $|\langle n|S_+(p)|s\rangle|^2$ is almost zero for $p<p_1(M)$.

The solid curves represent the lower bounds (1.5), (1.9), and (1.10) obtained from the analysis of the spin-wave continua.[1] The emergence of the soft mode at $p=p_3(M=1/4)=\pi/2$ in the longitudinal case [Fig. 1(a)] is

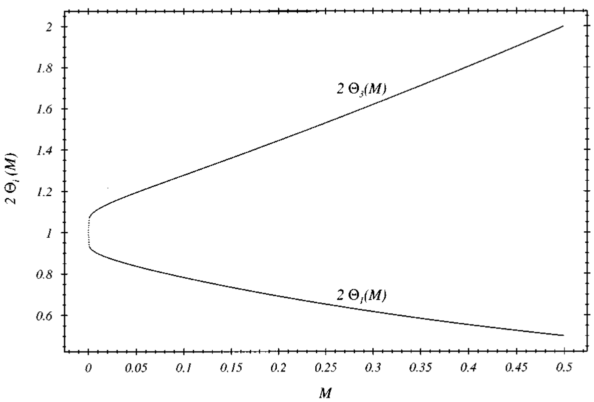

FIG. 2. The dependence of the scaled energy gaps $\theta_1(M)$ and $\theta_3(M)$ on the magnetization M.

clearly visible. Note that there are some excitations with small spectral weights below the bound (1.5) (for $p>3\pi/4$). We do not know whether the spectral weights will survive in the thermodynamical limit.

The lowest excitations in the transverse cases [Figs. 1(b) and 1(c)] are found at $p=\pi$ and at the field-dependent momenta

$$p_1^{\pm}(M)=p_1(M)\pm\frac{2\pi}{N}. \tag{2.3}$$

We have analyzed the finite-size dependence of the lowest excitation energies

$$\omega_3(p_3(M),M,N)=E(p=p_s+p_3(M),M=S/N,N)\\ -E(p_s,M=S/N,N), \tag{2.4a}$$

$$\omega_1(\pi,M,N)=E(p=p_s+\pi,M=(S+1)/N,N)\\ -E(p_s,M=S/N,N), \tag{2.4b}$$

$$\omega_\pm(p=p_1^{\pm}(M),M,N)=E(p_s+p_1^{\pm}(M),M=(S\pm1)/N,N)\\ -E(p_s,M=S/N,N). \tag{2.4c}$$

p_s denotes the ground-state momentum in the sector with total spin S; $p_s=0$ if $N+2S$ is a multiple of 4, and $p_s=\pi$ otherwise. The lowest-energy eigenvalues $E(p,M,N)$ with momentum p and spin S were computed on large systems ($N\leqslant 2048$) by solving the Bethe ansatz equations. The extrapolation of the energy differences (2.4) to the thermodynamical limit

$$\lim_{N\to\infty} N\omega_3(p_3(M),M,N)=\Omega_3(M),$$

$$\lim_{N\to\infty} N\omega_1(\pi,M,N)=\Omega_1(M), \tag{2.5a}$$

$$\lim_{N\to\infty} N\omega_\pm(p_1^{\pm}(M),M,N)=\Omega_1^{\pm}(M), \tag{2.5b}$$

obey the following relations:

$$\Omega_1^{\pm}(M)=\Omega_3(M)\pm\Omega_1(M). \tag{2.6}$$

Together with the spin-wave velocity $v(M)$,

$$2\pi v(M)=\lim_{N\to\infty} N[E(p_s+2\pi/N,M,N)-E(p_s,M,N)], \tag{2.7}$$

they define the scaled energy gaps

$$2\theta_a(M)=\frac{\Omega_a(M)}{\pi v(M)},\quad a=3,1, \tag{2.8a}$$

$$2\theta_1^{\pm}(M)=\frac{\Omega_1^{\pm}(M)}{\pi v(M)}=2[\theta_3(M)\pm\theta_1(M)]. \tag{2.8b}$$

The M dependence of the quantities $\theta_a(M)$, $a=3$ and 1, is shown in Fig. 2. It turns out that

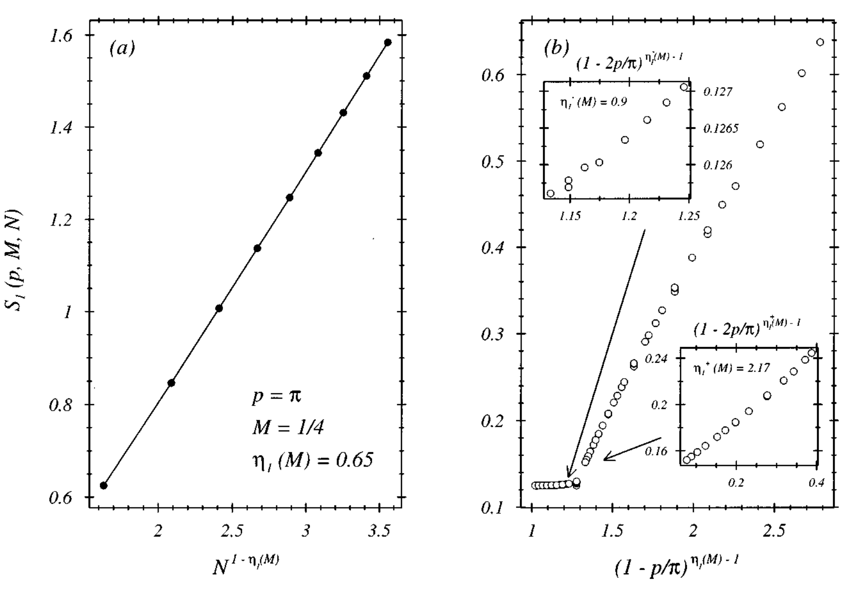

FIG. 3. The transverse static structure factor at $M=\frac{1}{4}$: (a) Finite-size behavior at $p=\pi$. (b) The momentum dependence $(1-p/\pi)^{\eta_1(M)-1}$ for $p\to\pi$, $(1-2p/\pi)^{\eta_1^-(M)-1}$ for $p\to\pi/2-0$ (inset upper left), and $|1-2p/\pi|^{\eta_1^+(M)-1}$ for $p\to\pi/2+0$ (inset, lower right).

$$2\,\theta_1(M) = \frac{1}{2\,\theta_3(M)} \tag{2.9}$$

in accord with the analytical result of Bogoliubov, Izergin, and Korepin.[7] In the limit $M \to \frac{1}{2}$ one finds $2\,\theta_3(M) = 1 + 2M$.[10] The dotted line in Fig. 2 near $M = 0$ indicates the logarithmic singularity

$$2\,\theta_3(M) \xrightarrow{M\to 0} 1 + \left(\ln\frac{1}{M^2}\right)^{-1}, \tag{2.10}$$

which was obtained by Bogoliubov, Izergin, and Korepin[10] by a perturbative approach to the Bethe ansatz equations.

III. CRITICAL BEHAVIOR OF THE STATIC STRUCTURE FACTORS AT THE SOFT-MODE MOMENTA

The static structure factors of the antiferromagnetic Heisenberg model in the presence of a magnetic field have been investigated in a previous numerical study on systems up to $N = 28$.[4] Meanwhile we have extended the system size to $N = 32$ and 36 at fixed magnetization $M = \frac{1}{4}$. We find the following features:

(1) The transverse structure factor at momentum $p = \pi$ diverges for $N \to \infty$. A power-law fit

$$S_1(\pi, M, N) \xrightarrow{N\to\infty} 0.503 N^{1-\eta_1(M)}, \tag{3.1}$$

to the finite system results for $N = 36$, 32, and 28 leads to the value $\eta_1(M = \frac{1}{4}) = 0.65$ for the critical exponent. The same exponent governs the approach to the singularity in the momentum p,

$$S_1(p, M, \infty) \xrightarrow{p\to\pi} 0.316\left(1 - \frac{p}{\pi}\right)^{\eta_1(M)-1}. \tag{3.2}$$

The finite-size dependence (3.1) is shown in Fig. 3(a). The momentum dependence can be seen in Fig. 3(b) where we have plotted $S_1(p = \pi, M = \frac{1}{4}, N)$ versus $(1 - p/\pi)^{\eta_1(M)-1}$ using the critical exponent determined in Fig. 3(a).

(2) The approach to the field-dependent soft mode $p_1(M) = 2\pi M$ in the transverse structure factor is shown in the upper left $[p \to p_1(M) - 0]$ and lower right $[p \to p_1(M) + 0]$ insets of Fig. 3(b). The numerical data behave as

$$S_1(p \to p_1(M) \pm 0, M, \infty) \sim \left|1 - \frac{p}{p_1(M)}\right|^{\eta_1^{\pm}(M)-1} \tag{3.3}$$

if the critical exponents are chosen to be $\eta_1^{+}(M = \frac{1}{4}) = 2.17$, $\eta_1^{-}(M = \frac{1}{4}) = 0.8 \ldots 1.2$. The uncertainty in $\eta_1^{-}(M = 1/4)$ reflects an instability in the fit to the numerical data. Note that the right-hand side of (3.3) diverges for $\eta_1^{-}(M = \frac{1}{4}) < 1$, but converges for $\eta_1^{-}(M = \frac{1}{4}) > 1$. An unambiguous determination of $\eta_1^{-}(M = \frac{1}{4})$ demands much larger systems than $N = 36$.

(3) The finite-size dependence of the longitudinal structure factors at $p = p_3(M)$,

$$S_3(p_3(M), M, N) \xrightarrow{N\to\infty} -0.124 N^{1-\eta_3(M)} + 0.308, \tag{3.4}$$

is shown in Fig. 4(a) for $M = \frac{1}{4}$, $p = p_3(M) = \pi/2$. A power-law fit to the finite system results with $N = 36$, 32, and 28 yields $\eta_3(M = \frac{1}{4}) = 1.51$. The same exponent governs the approach to the singularity from the left,

$$S_3(p \to p_3(M) - 0, M, N) \xrightarrow{N\to\infty} -0.312\left(1 - \frac{p}{p_3(M)}\right)^{\eta_3(M)-1} + 0.322, \tag{3.5}$$

as is demonstrated in Fig. 4(b). It is not so easy to decide whether a different exponent is needed to describe the approach to the singularity from the right. In the inset of Fig. 4(b) we plot the approach from the right versus $|1 - p/p_3(M)|^{\eta_3(M=1/4)-1}$.

The Fourier transform of the singularities in the static structure factors determines the large distance behavior of the corresponding spin-spin correlators

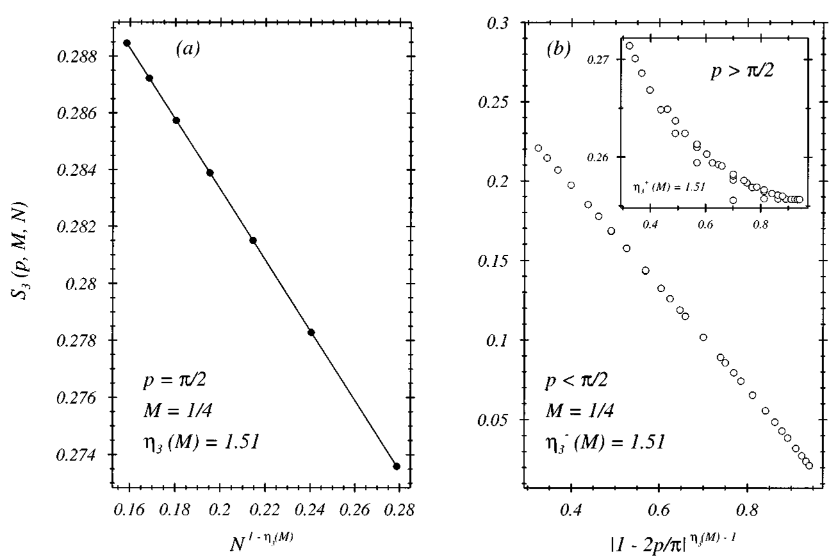

FIG. 4. The longitudinal static structure factor at $M = \frac{1}{4}$: (a) Finite-size behavior at $p = p_3(M) = \pi/2$. (b) The momentum dependence $|1 - 2p/\pi|^{\eta_3(M)-1}$ for $p < \pi/2$ and $p > \pi/2$ (inset), respectively.

TABLE II. The critical quantities $2\theta(M)$, $\eta(M)$, and $2[1-\alpha(M)]$ at $M=\frac{1}{4}$ and at the soft-mode momenta $p=p_3(M=\frac{1}{4})=\pi/2$, $p=p_1^+(M=\frac{1}{4})$, and $p=p_1^-(M=\frac{1}{4})$.

(a)	$2\theta_3(M)$	$\eta_3(M)$	$2[1-\alpha_3(p=\pi/2,M)]$	
$p=p_3(M)$	1.5312	1.51	1.54	
(b)	$2\theta_1(M)$	$\eta_1(M)$	$2[1-\alpha_+(p=\pi,M)]$	$2[1-\alpha_-(p=\pi,M)]$
$p=\pi$	0.6531	0.65	0.62	0.68
(c)	$2\theta_1^+(M)$	$\eta_1^+(M)$	$2[1-\alpha_+(p=p_1^+(M),M)]$	
$p=p_1^+(M)$	2.1843	2.17	2.40	
(d)	$2\theta_1^-(M)$	$\eta_1^-(M)$	$2[1-\alpha_-(p=p_1^-(M),M)]$	
$p=p_1^-(M)$	0.8781	0.8−1.2	2.1	

$$\langle s|S_1(0)S_1(x)|s\rangle \xrightarrow{x\to\infty} \cos(\pi x)\frac{A_1(M)}{x^{\eta_1(M)}} + \cos[p_1(M)x]\left(\frac{A_1^+(M)}{x^{\eta_1^+(M)}}+\frac{A_1^-(M)}{x^{\eta_1^-(M)}}\right), \quad (3.6a)$$

$$\langle s|S_3(0)S_3(x)|s\rangle - \langle s|S_3(0)|s\rangle^2 \xrightarrow{x\to\infty} \cos[p_3(M)x]\frac{A_3(M)}{x^{\eta_3(M)}}. \quad (3.6b)$$

Conformal field theory[9] predicts a relation between the critical exponents $\eta(M)$ in (3.6) and the scaled energy gaps (2.8)[7,8]

$$2\theta_a(M)=\eta_a(M), \quad a=3,1, \quad (3.7a)$$

$$2\theta_1^{\pm}(M)=\eta_1^{\pm}(M). \quad (3.7b)$$

A derivation of (3.7) is presented in the Appendix. A comparison of the left- and right-hand sides of (3.7) is presented in Table II.

IV. FINITE-SIZE SCALING ANALYSIS OF THE INFRARED SINGULARITIES

The Euclidean time representation

$$S_a(\tau,p,M,N)=\int_{\omega_a(p,M,N)}^{\infty} d\omega e^{-\omega\tau} S_a(\omega,p,M,N), \quad a=3,+,- \quad (4.1)$$

is most suited to study finite-size effects in the dynamical structure factors (1.2). The singularities in the static structure factors $S_a(\tau=0,p,M,N)$ at the soft-mode momenta originate from the infrared singularities in the dynamical structure factors. In the combined limit

$$\tau\to\infty, \quad N\to\infty, \quad (4.2)$$

keeping fixed the scaling variables

$$z_a(p,M)\equiv\tau\omega_a(p,M,N), \quad a=3,+,-, \quad (4.3)$$

the low-frequency part at the soft-mode momenta $p=\pi, p=p_1(M)\pm 2\pi/N, p=p_3(M)$ is projected out. We therefore expect here to see signatures for the infrared singularities directly. Let us assume that the emergence of the infrared singularities on finite systems can be described by a finite-size scaling ansatz

$$S_a(\omega,p,M,N)=\omega^{-2\alpha_a(p,M)} g_a(\omega/\omega_a(p,M,N), n_a(p,M,N)), \quad a=3,+,-. \quad (4.4)$$

The scaling functions g_a are supposed to depend only on the scaled excitation energies $\omega/\omega_a(p,M)$ and the variable

$$n_a(p,M,N)=[p-p_a(M)]N/(2\pi), \quad (4.5)$$

which describes the approach to the soft-mode momenta. Ansatz (4.4) induces the following finite-size scaling behavior of the Euclidean time representation (4.1) in the combined limit (4.2) and (4.3):

$$\tau^{1-2\alpha_a(p,M)} S_a(\tau,p,M,N)=G_a(z_a(p,M),n_a(p,M,N)) \times\exp[-z_a(p,M)]. \quad (4.6)$$

The two scaling functions on the right-hand sides of Eqs. (4.4) and (4.6) are related via

$$G(z,n)=z^{1-2\alpha}\int_1^{\infty} dx\; e^{-(x-1)z} g(x,n). \quad (4.7)$$

Based on our numerical results for $S_a(\tau,p,M,N)$ at $M=\frac{1}{4}$, $a=3,+$, $N=16,20, \ldots ,36$, and $a=-$, $N=16,20, \ldots ,32$ at the soft-mode momenta, we will now test the validity of the finite-size scaling ansatz (4.6).

Let us start with the longitudinal structure factor at the soft mode $p=p_3(M=\frac{1}{4})=\pi/2$. In this case the variable (4.5) is $n_3(p=\pi/2,M=\frac{1}{4})=0$. The left-hand side of (4.6) versus the scaling variable $z_3(p=\pi/2,M=\frac{1}{4})$ is shown in Fig. 5(a) for the following values of $\alpha_3(p=\pi/2,M=\frac{1}{4})=0.22$, 0.23, and 0.234. For $z_3\geqslant 0.4$ [the inset of Fig. 5(a)], the finite system results coincide best if

$$\alpha_3(p=\pi/2,M=\tfrac{1}{4})=0.23. \quad (4.8)$$

Therefore, this is the expected critical exponent for the infrared singularity in the longitudinal structure factor. Deviations from this value for α_3 on the left-hand side of (4.6) obviously lead to a violation of finite-size scaling. It is remarkable that finite-size scaling [with the exponent $\alpha_3(p=\pi/2,M=\frac{1}{4})=0.23$] persists for all values $z_3\geqslant 0.4$. In

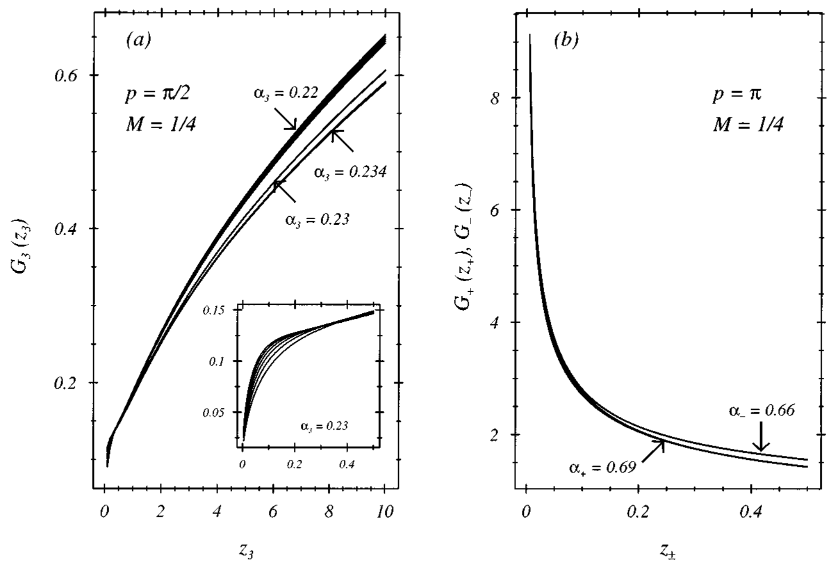

FIG. 5. Test of finite-size scaling for the infrared singularities in the dynamical structure factors at $M=\frac{1}{4}$: (a) The longitudinal case at the soft mode $p=p_3(M)=\pi/2$. The inset resolves scaling violations for small values of the scaling variable z_+. (b) The transverse cases at $p=\pi$.

the limit $z_3 \to \infty$ the first excitation alone survives and we can conclude on the finite-size dependence of the transition probability

$$|\langle n=1|S_3(p=\pi/2)|s\rangle|^2 \xrightarrow{N\to\infty} N^{2\alpha_3-1}. \tag{4.9}$$

In other words, the critical exponent α_3 for the infrared singularity can by read off the finite-size dependence of the transition probability for the first excitation. Indeed this feature is predicted by conformal field theory[7] [cf. (A9) in the Appendix].

Next we turn to the infrared singularities of the transverse structure factors $S_\pm(\omega,p=\pi,M=\frac{1}{4})$. As can be seen from Fig. 5(b), finite-size scaling is found for the following choice of the critical exponents:

$$\alpha_+(p=\pi,M=\tfrac{1}{4})=0.69, \tag{4.10a}$$

$$\alpha_-(p=\pi,M=\tfrac{1}{4})=0.66. \tag{4.10b}$$

In contrast to the longitudinal case, finite-size scaling can be observed here for all values of the scaling variables z_+, z_-.

Finally in Figs. 6(a) and 6(b) we present tests of the finite-size scaling for the transverse structure factors $S_\pm(\tau,p=\pi/2\pm 2\pi/N,M=\frac{1}{4},N)$ if we approach the field-dependent soft mode $p_1(M=\frac{1}{4})=\pi/2$ from the left $(p=\pi/2-2\pi/N)$ and from the right $(p=\pi/2+2\pi/N)$, respectively. The critical exponents are found to be

$$\alpha_+(p=\pi/2+2\pi/N,M=\tfrac{1}{4})=-0.20, \tag{4.11a}$$

$$\alpha_-(p=\pi/2-2\pi/N,M=\tfrac{1}{4})=-0.05. \tag{4.11b}$$

Finite-size scaling works quite well for S_+ for large and small values of the scaling variable z_+, as can be seen from the inset in Fig. 6(a). This is not the case for S_-. Here finite-size scaling breaks down for small values of z_- as is demonstrated in the inset of Fig. 6(b). The critical exponent $\alpha_-(p=\pi/2-2\pi/N,M=\frac{1}{4})=-0.05$ results from the finite-size scaling analysis for large values of z_-, where the transition probability for the first excitation is projected out and has the following finite-size dependence:

$$|\langle n=1|S_-(p=\pi/2-2\pi/N)|s\rangle|^2 \xrightarrow{N\to\infty} N^{2\alpha_- -1}. \tag{4.12}$$

V. DISCUSSION AND CONCLUSIONS

In the presence of a uniform field, the one-dimensional antiferromagnetic Heisenberg model is critical in the following sense: The excitation spectrum is gapless at the momenta $p=0$, $p=\pi$, $p=p_3(M)=\pi(1-2M)$, and $p=p_1(M)=\pi 2M$. In this paper we have tried to answer the following question: Is conformal field theory applicable to describe the low-energy excitations at these momenta? To answer this question we have determined (1) the scaled energy gaps $2\theta(M)$, defined through (2.4)–(2.8); (2) the critical exponents $\eta(M)$ for the singularities (3.2), (3.3), and (3.5) in the static structure factors; and (3) the exponents $\alpha(M)$ for the infrared singularities (4.4) in the dynamical structure factors. A compilation of the various critical quantities for $M=\frac{1}{4}$ is given in Table II.

The predictions of conformal field theory are reviewed in the Appendix. In particular the following relation is expected to hold:

$$2\theta(M)=\eta(M)=2[1-\alpha(p,M)]. \tag{5.1}$$

Looking at Table II we find the following.

(a) The critical quantities $2\theta_3(M=\frac{1}{4})$, $\eta_3(M=\frac{1}{4})$, and $2-2\alpha_3(p=\pi/2,M=\frac{1}{4})$ agree within the numerical uncertainty. Moreover, the critical exponent $\alpha_3(p=\pi/2,M=\frac{1}{4})$ also governs the finite-size dependence of the transition probability for the lowest excitation (4.9). We therefore conclude that the excitations in the longitudinal structure factors at the soft mode $p_3(M)=\pi(1-2M)$ are correctly described by conformal field theory.

(b) The critical quantities $2\theta_1(M=\frac{1}{4})$, $\eta_1(M=\frac{1}{4})$, $2-2\alpha_+(p=\pi,M=\frac{1}{4})$, and $2-2\alpha_-(p=\pi,M=\frac{1}{4})$ agree within numerical uncertainties. In both cases the finite-size

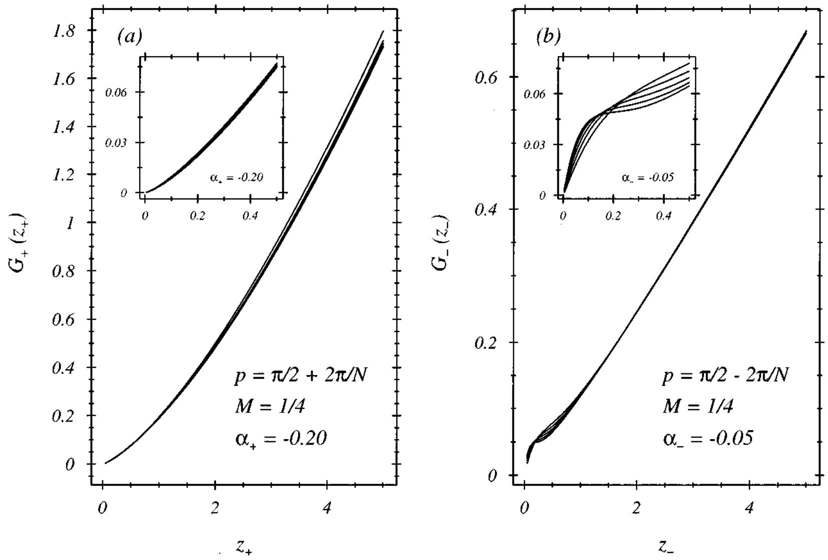

FIG. 6. Test of finite-size scaling for the infrared singularities in the transverse structure factors at $M=\frac{1}{4}$: (a) The transverse case S_+ at the soft mode $p=p_1^+(M)=\pi/2+2\pi/N$. The inset shows a magnification for small values of the scaling variable z_+. (b) The transverse case S_- at the soft mode $p=p_1^-(M)=\pi/2-2\pi/N$. The inset resolves scaling violations for small values of the scaling variable z_-.

dependence of the transition probability for the lowest excitation is in accord with the prediction of conformal field theory.

(c) The critical quantities $2\theta_1^+(M=\frac{1}{4})$ and $\eta_1^+(M=\frac{1}{4})$ agree within numerical uncertainties, and deviate by about 15% from the exponent $2[1-\alpha_+(p=\pi/2+2\pi/N,M=\frac{1}{4})]$.

(d) The scaled energy gap $2\theta_1^-(M=\frac{1}{4})$ agrees with the critical exponent $\eta_1^-(M=\frac{1}{4})$—within the large numerical uncertainty—but strongly deviates by more than a factor of 2 from the exponent $2(1-\alpha_-[\pi/2-1/(2N),M=\frac{1}{4}])$, which we extracted from the finite-size scaling analysis of the infrared singularity in the transverse structure factor S_- at the soft mode $p=p_1(M)-2\pi/N,M=\frac{1}{4}$. It was demonstrated in Fig. 6(b) that finite-size scaling only works for large values of the variable z_-, where the first excitation alone contributes. Therefore, the exponent $2[1-\alpha(\pi/2-2\pi/N,M=\frac{1}{4})]$ is fixed by the finite-size behavior (4.12) of the transition probability for the first excitation. The exponent is definitely different from the scaled energy gap $2\theta_1^-(M=\frac{1}{4})$.

It is worthwhile to note that in the cases (a), (b), and (c), where we find agreement of our numerical results with prediction (5.1) of conformal field theory, the spectral weight of the excitations is concentrated at low frequencies. This can be seen directly for case (b) ($p=\pi$) in the left-hand part of Table I. In contrast, the right-hand part of Table I shows the widespread distribution of the spectral weight for case (d). Here we were not able to establish identity (5.1).

ACKNOWLEDGMENTS

We are indebted to Professor K. Fabricius, who made available to us the exact numerical results in the upper part of Table I. We thank Professor G. Müller for helpful comments on this paper. M.K. gratefully acknowledges support by the Max Kade Foundation. C.G. was supported by the Graduiertenkolleg ''Feldtheoretische und numerische Methoden in der Elementarteilchen Physik und Statistischen Physik.''

APPENDIX: CRITICAL EXPONENTS IN CONFORMAL FIELD THEORY

In the absence of a magnetic field the spin-$\frac{1}{2}$ Heisenberg model is known to be conformal invariant. Switching on the magnetic field, the rotational invariance is broken explicitly. Nevertheless the system remains gapless. Let us assume that the low-energy physics of the model is still governed by conformal field theory. Then the dominant contribution to the long distance asymptotics of the zero-temperature dynamical correlation functions in the infinite $x-t$ plane is correctly described as[10]

$$\langle s|S_a(0,0)S_a(x,t)|s\rangle-\langle s|S_a(0,0)|s\rangle^2 = e^{ixp_a(M)}\frac{A_a(M)}{[x+v(M)t]^{2\Delta_a(M)}[x-v(M)t]^{2\bar{\Delta}_a(M)}}. \tag{A1}$$

$v(M)$ is the spin-wave velocity defined in (2.7), and $\Delta_a(M)$ and $\bar{\Delta}_a(M)$ are the conformal dimensions of the operator $S_a(x,t)$. The dynamical structure factor $S_a(\omega,p)$ is just the Fourier transform of (A1) with an appropriate regularization. The latter can be achieved by giving an infinitesimal imaginary part to the spin-wave velocity $v(M)$. Standard methods yield

$$S_a(\omega,p)\sim\{\omega\mp v(M)[p-p_a(M)]\}^{2\Delta_a(M)+2\bar{\Delta}_a(M)-2}, \tag{A2}$$

near the singularities

$$\omega\approx\pm v(M)[p-p_a(M)]. \tag{A3}$$

Equation (A2) is obtained if we first consider the case $\Delta_a(M)+\bar{\Delta}_a(M)>\frac{1}{2}$ and then continue analytically. A conformal transformation to a strip geometry of width N tells us how the conformal dimensions $\Delta_a(M)$ and $\bar{\Delta}_a(M)$ are related to the energy and momentum of the lowest excitation $|1\rangle$, provided that the transition matrix element $\langle s|S_a(0,0)|1\rangle$ does not vanish:

$$2\Delta_a(M)=\theta_a(M)+n_a\,, \tag{A4a}$$

$$2\overline{\Delta}_a(M)=\theta_a(M)-n_a\,, \tag{A4b}$$

where

$$n_a=[p-p_a(M)]\frac{N}{2\pi}. \tag{A5}$$

Therefore we conclude that the infrared singularity of the dynamical structure factor,

$$S_a(\omega,p)\sim\frac{1}{\{\omega\pm v(M)[p-p_a(M)]\}^{2\alpha_a(M)}}, \tag{A6}$$

is independent of n_a:

$$\alpha_a(M)=1-\theta_a(M). \tag{A7}$$

The critical exponent $\eta_a(M)$ can be read off directly from (A1):

$$\eta_a(M)=2\Delta_a(M)+2\overline{\Delta}_a(M)=2\theta_a(M). \tag{A8}$$

In (A1) it is assumed that the coefficient $A_a(M)$ is nonvanishing. From the conformal transformation to the strip geometry, a relation between $A_a(M)$ and the transition matrix element can be derived:

$$A_a(M)=\lim_{N\to\infty}\left[2\left(\frac{N}{\pi}\right)^{2\theta_a(M)}e^{i\pi n_a}|\langle s|S_a(x,0)|1\rangle|^2\right]. \tag{A9}$$

Therefore, the matrix element is expected to scale as

$$|\langle s|S_a(x,0)|1\rangle|^2\sim N^{2\alpha_a(M)-2}. \tag{A10}$$

If a finite-size analysis of these critical exponents reveals that

$$\theta_a(M)<1-\alpha_a(M), \tag{A11}$$

the coefficient $A_a(M)$ vanishes. In this case the expression (A1) does not represent the dominant contribution to the dynamical structure factor.

*Electronic address: muetter@wpts0.physik.uni-wuppertal.de

[1] G. Müller, H. Thomas, G. Beck, and J.C. Bonner, Phys. Rev. B **24**, 1429 (1981); G. Müller, H. Thomas, M.W. Puga, and G. Beck, J. Phys. C **14**, 3399 (1981).

[2] C.N. Yang and C.P. Yang, Phys. Rev. **151**, 258 (1966); R.B. Griffiths, Phys. Rev. **133**, A768 (1964); J.C. Bonner and M.E. Fisher, *ibid.* **135**, A640 (1964).

[3] J.B. Parkinson and J.C. Bonner, Phys. Rev. B **32**, 4703 (1985); M.D. Johnson and M. Fowler, *ibid.* **34**, 1728 (1986).

[4] M. Karbach, K.-H. Mütter, and M. Schmidt, J. Phys. Condens. Matter **7**, 2829 (1995); M. Schmidt, C. Gerhardt, K.-H. Mütter, and M. Karbach, *ibid.* **8**, 553 (1996).

[5] A. Fledderjohann, M. Karbach, K.-H. Mütter and P. Wielath, J. Phys. Condens. Matter **7**, 8993 (1995).

[6] V.S. Viswanath, S. Zhang, J. Stolze, and G. Müller, Phys. Rev. B **49**, 9702 (1994); V.S. Viswanath and G. Müller, *The Recursion Method - Application to Many Body Dynamics*, Springer Lecture Notes in Physics Vol. 23 (Springer-Verlag, New York, 1994).

[7] N.M. Bogoliubov, A.G. Izergin, and N. Y. Reshetikhin, J. Phys. A **20**, 5361 (1987).

[8] H.J. Schultz and T. Ziman, Phys. Rev. B **33**, 6545 (1986).

[9] J.L. Cardy, Nucl. Phys. B **279**, 186 (1986) .

[10] N.M. Bogoliubov, A.G. Izergin, and V.E. Korepin, Nucl. Phys. B **275**, 687 (1986).